The effect of boron addition on the atomic structure and microwave magnetic properties of FeGaB thin films

Jinsheng Gao,[1,a)] Aria Yang,[1] Yajie Chen,[1] J. P. Kirkland,[2] Jing Lou,[1] Nian X. Sun,[1] Carmine Vittoria,[1] and Vincent G. Harris[1]
[1]*Department of Electrical and Computer Engineering, Center for Microwave Magnetic Materials and Integrated Circuits, Northeastern University, Boston, Massachusetts 02115, USA*
[2]*SFA Inc., Landover, Maryland 20785, USA*

(Presented 11 November 2008; received 18 September 2008; accepted 17 November 2008; published online 11 March 2009)

Varying amounts of boron were added to the host FeGa alloy to investigate its impact upon local atomic structure and magnetic and microwave properties. The impact of B upon the local atomic structure in FeGaB films was investigated by extended x-ray absorption fine structure (EXAFS) analysis. The EXAFS fitting results revealed a contraction of lattice parameters with the introduction of B. The Debye–Waller factor determined from EXAFS fitting increases as a function of boron addition and abruptly changes during the structural evolution from crystalline to amorphous that occurs near 9% B. Upon the onset of this transition the static and microwave magnetic properties became exceptionally soft, with values of coercivity and ferromagnetic linewidth reducing to less than 1 Oe and 25 Oe, respectively. © *2009 American Institute of Physics*.
[DOI: 10.1063/1.3072027]

I. INTRODUCTION

FeGa alloys are soft magnetic materials with saturation magnetostriction constants of ~400 ppm for single crystals[1] and ~275 ppm for polycrystalline samples.[2] Additionally, these alloys have saturation magnetization values of ~18 kG and saturation fields on the order of 100 Oe (Ref. 3). However, because of high losses at microwave frequencies and subsequent large ferromagnetic resonance (FMR) linewidths,[4] realization of FeGa-based microwave devices has not been forthcoming. Recently, incorporation of the metalloid element boron into FeGa alloys[5–8] was shown to lead to excellent soft magnetic properties with coercive fields <1 Oe, high $4\pi M_s$ of 17.5 K Gauss, narrow FMR linewidths of 16–20 Oe at *X*-band, and a saturation magnetostriction constant of ~70 ppm. The combination of these properties makes FeGaB films suitable for use in tunable magnetoelectric RF-microwave devices.

In this paper, we investigate the impact of B upon the local atomic structure in $(Fe_{0.80}Ga_{0.20})_{1-x}B_x$ films where x ranges from 0–0.21 using extended x-ray absorption fine structure (EXAFS) analysis. Because EXAFS offers both element specificity and local structure sensitivity, it is an ideal probe for this purpose. Atomic near-neighbor bond distances, lattice parameters, and other local structure properties were determined by multiple scattering least-squares fitting. The structural, magnetic, and microwave properties of the FeGaB films, including coercivity, anisotropy field, and FMR linewidth, were measured and correlated with reveal the role of B in this new alloy system.

II. EXPERIMENT

$(Fe_{0.80}Ga_{0.20})_{1-x}B_x$ films with B contents (x) ranging from 0 to 0.21 were magnetron co-puttered onto silicon substrates from individual 2.0 inch diameter targets of $Fe_{80}Ga_{20}$ and boron. The substrate was exposed to an *in situ* applied magnetic field of ~100 Oe to form an induced uniaxial in-plane magnetic anisotropy. By changing the boron sputter gun power, the boron concentration of the FeGaB films was varied while maintaining the $Fe_{80}Ga_{20}$ gun power at 50 W. FeGaB films were deposited in a 3 mTorr Ar atmosphere at a rate of 60 Å/min with a base pressure of less than 1×10^{-7} Torr. The thickness was measured to be ~100 nm by a surface profilometer.

dc magnetic properties of the FeGaB films were measured by vibrating sample magnetometry. Microwave properties were collected by a customer-made permeameter with a bandwidth of 0.05–5 GHz and an *X*-band FMR spectrometer. The crystal structure of the FeGaB films was determined by x-ray diffractometry. The resistivity was measured and calculated using a collinear four point probe method. Some of these properties have been previously reported in Ref. 8.

Iron *K* edge x-ray absorption spectra were collected at the National Synchrotron Light Source using beamline X23B. The design and optical performance of this beamline is presented in Ref. 9. Data collection was performed in fluorescence yield at room temperature using a gas ionization detector with a combination of N_2 and Ar as the working gases. Three to five sets of data for each sample were merged during analysis to improve the statistical robustness of the extended fine structure fitting. The experimental data in energy space were reduced to photoelectron wave vector (k) space and then Fourier transformed (FT) to radial coordinates following established EXAFS analysis procedures.[10] The EXAFS data were FT using a k-range of 2.0–12.0 Å for crystal samples and 2.0–11.0 Å for amorphous. FT data sets were merged in k space whereas the least-squares fitting for crystal samples was performed in radial space over the range 1.5–4.9 Å. For amorphous samples, only the first coordination shell is fitted in radial space range of 1.5–3 Å. Taking into account of the asymmetry in the radial distribution func-

a)Electronic mail: gao.j@neu.edu.

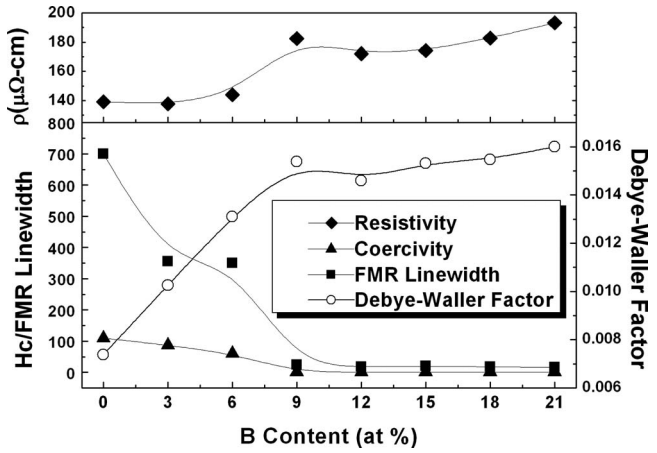

FIG. 1. Room temperature electrical resistivity (top panel) for FeGaB films for different B concentrations (0~21%). DW coefficients (with third cumulant), coercive field and FMR linewidths (bottom panel) for FeGaB films with different B concentrations (0~21%).

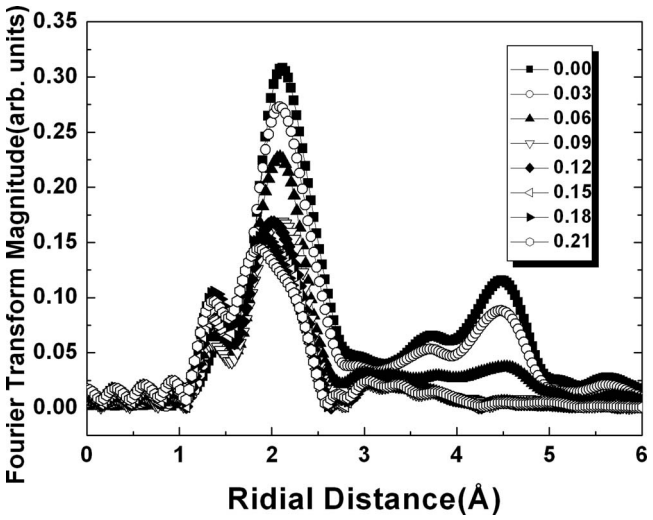

FIG. 2. Fourier transform (FT) of Fe *K*-edge EXAFS data of FeGaB films with B contents ranged from 0 to 0.21.

tion of amorphous alloy, we have carried out Gaussian approximation fitting procedure with high order cumulant C_3 representing the big disorder in the structure. The EXAFS fitting with $C_3=0$ is also carried out for comparison. These fits were performed using the Athena and Artemis codes of Ravel and Newville.[11] Theoretical EXAFS standards were generated by FEFF-6.[12]

III. RESULTS AND DISCUSSION

A summary of magnetic and microwave properties of FeGaB films having various boron content is shown in Fig. 1. The coercivity of the FeGaB films was significantly reduced from ~110 Oe for FeGa films to less than 1 Oe with 9% born addition and reaches a minimum value of 0.4 Oe at 21%. The effective in-plane anisotropy field, H_k, which is induced by the application of the magnetic field during deposition, similarly dropped from 120 to 30 Oe at 9% boron and reached ~15 Oe at 21%. FMR measurements of FeGaB films were carried out using an external field applied parallel to the in-plane easy axis. FeGa films typically have FMR linewidths of about 700 Oe.[4] With the incorporation of B, the FMR linewidth drops dramatically to 24 Oe at 9% boron addition, and remains below 20 Oe at 12%, and reaches a minimum of 16 Oe at 21%. This trend is illustrated in Fig. 1. The electrical resistivity at room temperature was measured to increase from ~140 $\mu\Omega$ cm in the crystalline state (<9% boron) to ~180 $\mu\Omega$ cm in the amorphous state (>9% boron) which is also shown in Fig. 1. Such high electrical resistivity suggests that eddy current losses in this alloy system would be less than other soft magnetic alternatives. Also, plotted in the Fig. 1 are the EXAFS-determined Debye–Waller (DW) coefficients for the first transition metal-metal bond determined by our best fit EXAFS model. In this instance, the DW parameter reflects both the static and temperature-dependent atomic displacements about the mean bond distance. It is a very useful parameter in assessing the degree of atomic structure disorder relative to the absorbing ion specie.

The EXAFS analysis was performed in order to better understand the role of the boron ion in altering the local structure of transition metal ions in FeGaB films and its subsequent impact on the dc and microwave magnetic properties. The FT EXAFS spectra of FeGaB with varying amounts of boron are presented in Fig. 2. The radial positions of the FT peaks represent the distance between the absorbing ions and their near neighbors plus a photoelectron phase shift. The amplitude of the FT peaks reflects both the coordination of ions at those radial distances together with the dynamic and static atomic disorder. The Fourier transform peaks seen in Fig. 2 have been identified to correspond with atomic pair correlations of Fe-Fe/Ga within the FeGaB bcc unit cell. The FT peak amplitudes reduce as the boron addition increases. When the B percentage reaches ~9%, the peak amplitude drops dramatically, corresponding to the structural phase change from crystalline to amorphous; a similar trend was observed in XRD spectra of Ref. 8, however, XRD is much less sensitive to the detection of local structural disorder. With the addition of B atoms, the first FT peak at a radial coordinate near ~2 Å, representing the bond distance along with contribution from the amorphous disorder between Fe ions and their near neighbor Fe/Ga ions, shifts to lower radial distances. This radial distance decrease has been observed in other systems in which crystalline to amorphous transitions occur[13–15] and usually corresponds to the contraction of

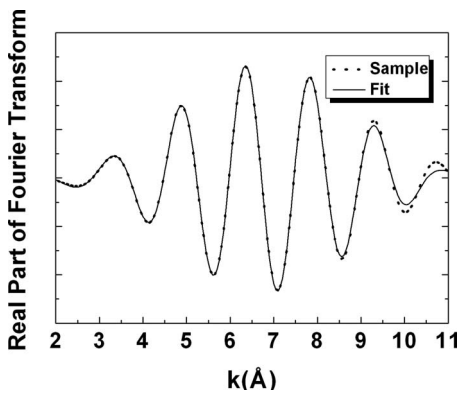

FIG. 3. FT of first shell of Fe *K*-edge EXAFS data and best fit (with the third cumulant) for $(Fe_{0.80}Ga_{0.20})_{1-x}B_x$ film where $x=0.09$.

TABLE I. Structural parameters determined from the multiple scattering nonlinear least-squares fitting with and without the third cumulant of EXAFS data of $(Fe_{0.80}Ga_{0.20})_{1-x}B_x$ films. The uncertainties in the last significant digit are shown in parenthesis. NN stands for nearest neighbor.

B content (x)	NN bond distance of Fe-Fe/Ga (Å)	Debye–Waller factor of first metal-metal bond ($Å^2$)	Third cumulant ($Å^3$)	Lattice parameter (Å)
0.00	2.482(6)	0.007(1)	0	2.899(2)
0.03	2.482(5)	0.010(1)	0	2.896(1)
0.06	2.470(6)	0.013(2)	0	2.891(1)
0.09	2.479(5)	0.019(1)	0	
	2.51(1)	0.015(1)	0.0004(2)	
0.12	2.465(4)	0.017(2)	0	
	2.52(1)	0.014(1)	0.0006(3)	
0.15	2.464(5)	0.019(2)	0	
	2.54(2)	0.015(1)	0.0008(4)	
0.18	2.454(4)	0.017(2)	0	
	2.55(2)	0.015(1)	0.0015(5)	
0.21	2.442(4)	0.019(2)	0	
	2.56(2)	0.015(1)	0.0016(5)	

bonds coinciding with the collapse of rigid bonds and bond angles inherent to crystalline lattices. As we noted earlier, in the amorphous system, we considered the asymmetry of the radial distribution function and added a high order cumulant (C_3) representing the big disorder in the fit model. With the more general EXAFS model considering the large disorder, the DW increases abruptly when the structure phase changes from crystalline to amorphous. We also found C_3 linearly increases with the addition of B contents indicating the escalation of the disorder. Additionally, we need to point out the fact that in the fitting analysis, the approach to substitute Fe/Ga ions in the first coordination shell with B ions in the FEFF model did not improve the fits. These evidences suggest the B ions localize in the interstitial sites and increased the disorder substantially.

Figure 3 includes the best fit and the experimental EXAFS data for the real part of inverse Fourier transform of the first shell of Fe K-edge spectra for the $x=0.09$ film. The quality of the fit is representative of the other data sets. The fitting results determined from the best fits, including lattice parameters, bond distances between Fe ions and near neighbors, and the DW coefficients are presented in Table I. The comparison between best fit and experimental data is reflected in R factors ranging from 0.02 to 0.08: values which are considered indicative of a constrained model that contains the essential attributes of the experimental atomic arrangement. The Fe-Fe/Ga bond distances are found to reduce from 2.482(6) Å to 2.470(6) Å in the crystal samples with increased boron content. The lattice parameter is measured to contract from 2.899(2) to 2.891(1) with the addition of boron before the structural transitions to the amorphous phase. The DW coefficients of the first Fe-Fe/Ga atomic bond, determined from the EXAFS best fits, increases sharply from 0.007 $Å^2$ to 0.015 $Å^2$ with boron content increasing from 0% to 9%. These results are plotted in Fig. 1 and again confirm the change in structure from the crystalline to amorphous phase near $x=0.09$. From Fig. 1, we observe the atomic disorder evidenced by DW coefficients and the third cumulant C_3 is found to inversely correlate with the RF and dc losses, represented by reduced FMR linewidths and coercivity. This disorder is on the atomic level and does not effectively pin domain walls, which maintains the films' magnetically soft properties. As a result, the dramatically improved magnetic and microwave properties make these FeGaB films suitable for many RF-microwave applications.

ACKNOWLEDGMENTS

This research was performed in part at the National Synchrotron Light Source at the Brookhaven National Laboratory which is sponsored by the Department of Energy. This research was also supported by the National Science Foundation under Grant No. DMR 0400676 and the Office of Naval Research under Grant No. N00014–05–10349.

[1] A. E. Clark, M. Wun-Fogle, J. B. Restorff, and T. A. Lograsso, Mater. Trans., JIM **43**, 881 (2002).
[2] N. Srisukhumbowornchai and S. Guruswamy, J. Appl. Phys. **90**, 5680 (2001).
[3] A. E. Clark, J. B. Restorff, M. Wun-Fogle, T. A. Lograsso, and D. L. Schlagel, IEEE Trans. Magn. **36**, 3238 (2000).
[4] A. Butera, J. Gómez, J. L. Weston, and J. A. Barnard, J. Appl. Phys. **98**, 033901 (2005).
[5] Y. Gong, C. Jiang, and H. Xu, Acta Metall. Sin. **42**, 830 (2006).
[6] T. Kubota and A. Inoue, Mater. Trans. **45**, 199 (2004).
[7] K. Fukamichi, T. Satoh, and T. Masumoto, J. Magn. Magn. Mater. **31–34**, 1589 (1983).
[8] J. Lou, R. E. Insignares, Z. Cai, K. S. Ziemer, M. Liu, and N. X. Sun, Appl. Phys. Lett. **91**, 182504 (2007).
[9] R. A. Neiser, J. P. Kirkland, W. T. Elam, and S. Sampath, Nucl. Instrum. Methods Phys. Res. A **266**, 220 (1988).
[10] D. E. Sayers and B. A. Bunker, *X-ray Absorption: Principles, Applications, Techniques of EXAFS, SEXAFS and XANES*, edited by D. C. Konigsberger and R. Prins (Wiley, New York, 1988).
[11] B. Ravel and M. Newville, J. Synchrotron Radiat. **12**, 537 (2005).
[12] J. J. Rehr and R. C. Albers, Rev. Mod. Phys. **72**, 621 (2000).
[13] V. G. Harris, D. J. Fatemi, K. B. Hathaway, Q. Huang, A. Mohan, and G. J. Long, J. Appl. Phys. **85**, 5181 (1999).
[14] M. Tamoria, E. E. Carpenter, M. M. Miller, J. H. Claassen, B. N. Das, R. M. Stroud, L. K. Kurihara, R. K. Everett, M. A. Willard, A. C. Hsiao, M. E. McHenry, and V. G. Harris, IEEE Trans. Magn. **37**, 2264 (2001).
[15] A. Corrias, G. Navarra, M. F. Casula, S. Marras, and G. Mountjoy, J. Phys. Chem. B **109**, 13964 (2005).